applied sciences

MDPI

Article

Seismic Wave Propagation Characteristics and Their Effects on the Dynamic Response of Layered Rock Sites

Lihu Dong [1], Danqing Song [2,*] and Guangwei Liu [3]

[1] School of Electrical Engineering, Shenyang University of Technology, Shenyang 110870, China; donglh2019@smail.sut.edu.cn
[2] State Key Laboratory of Hydroscience and Engineering, Department of Hydraulic Engineering, Tsinghua University, Beijing 100084, China
[3] College of Mining Engineering, Liaoning Technical University, Fuxin 123000, China; liuguangwei@lntu.edu.cn
* Correspondence: songdq2019@mail.tsinghua.edu.cn; Tel./Fax: +86-1326-990-9592

Abstract: To investigate the seismic response of layered rock sites, a multidomain analysis method was proposed. Three finite element models with infinite element boundaries for layered sites were analysed. The results of this multidomain analysis show that stratum properties and elevation have an impact on wave propagation characteristics and the dynamic response of layered sites. Compared with the rock mass, the overlying gravel soil has a greater dynamic amplification effect at the sites. A time domain analysis parameter $PGA_{(IMF)}$ was proposed to analyse the effects of different strata on the seismic magnification effect of layered sites, and its application was also discussed in comparison with PGA. According to the frequency domain analysis, the interface of the rock mass strata has a low impact on the Fourier spectrum characteristics of the sites, but gravel soil has a great magnification effect on the spectrum amplitude in the high-frequency band ($\geq$30 Hz) of waves. Moreover, the stratum properties have a great influence on the shape and peak value of the Hilbert energy and marginal spectrum at layered sites. When waves propagate from hard rock to soft rock, the peak value of the Hilbert energy spectrum changes from single to multiple peaks; then, in gravelly soil, the Hilbert energy spectral peak, its nearby amplitude and the amplitude in the high-frequency band (28–36 Hz) are obviously amplified. The frequency components and amplitude of the marginal spectrum become more abundant and larger from rock to gravelly soil in the high-frequency band (28–35 Hz).

Keywords: dynamic response; layered sites; spectral characteristics; multidomain analysis; seismic excitation

check for updates

Citation: Dong, L.; Song, D.; Liu, G. Seismic Wave Propagation Characteristics and Their Effects on the Dynamic Response of Layered Rock Sites. *Appl. Sci.* **2022**, *12*, 758. https://doi.org/10.3390/app12020758

Academic Editor: Daniel Dias

Received: 6 December 2021
Accepted: 5 January 2022
Published: 12 January 2022

Publisher's Note: MDPI stays neutral with regard to jurisdictional claims in published maps and institutional affiliations.

Copyright: © 2022 by the authors. Licensee MDPI, Basel, Switzerland. This article is an open access article distributed under the terms and conditions of the Creative Commons Attribution (CC BY) license (https://creativecommons.org/licenses/by/4.0/).

1. Introduction

Western China has been prone to earthquakes in recent decades; specifically, the Wenchuan earthquake in 2008 was the largest and most widely distributed earthquake disaster in China [1,2]. Earthquake disasters mainly involve damage directly caused by fault dislocation and damage caused by strong earthquakes [3–5]. The former is generally in the blind area of the earthquake, which is difficult to prevent, while the latter is mainly affected by geological conditions, as has been verified by the Wenchuan earthquake [6,7]. By contrast, the approximately 30 m-thick sand and pebble layer below China's Chengdu area effectively consumes the energy transmitted by seismic waves and reduces the impact of ground motion on the tall buildings above [8]. The geological conditions of sites, in short, have a great influence on their seismic response [9–13]. In Southwest China, many important buildings are built on different types of sites with complex geological structures; in particular, layered sites are a common type of building site. Due to the complex geological materials and structures in layered sites, the seismic response of the sites has been complicated [14–17]. Therefore, the seismic response of layered sites has become an important research topic in geotechnical engineering.

The seismic response of sites has an important effect on the stability of the overlying buildings [18], making it essential to study their dynamic response characteristics. Since Wood realised the influence of site conditions on the seismic dynamic response from the 1928 San Francisco earthquake, researchers have been investigating the seismic response characteristics of stratified sites using quantitative methods due to the lack of measured data on field seismic responses [19,20]. With the collection and accumulation of seismic damage data from previous earthquakes, the seismic response of sites has attracted increasing attention. Many scholars have obtained meaningful conclusions through studies using the empirical method of strong vibration observation, analytical analysis and numerical simulation [21–23]. Celebi studied the intensity anomalies in the Chile and Mexico earthquakes in 1985 and California earthquakes in 1987 by using the traditional spectral ratio method based on the main and aftershock acceleration histories of earthquakes and thereby obtained the topography and soil layer amplification effect [24]. Based on the aftershock records of the Northridge Earthquake in 1994, Bonilla et al. used the traditional spectral ratio method, generalised linear inversion method and H/V method to study the field amplification effect in the intensity anomaly area of the San Fernando Valley in California [25]. Tsuda et al. analysed the Kanto Basin by the generalised linear inversion method and found that the intensity anomaly area was caused by soil layer amplification [26]. In addition, horizontally stratified sites are common geological bodies in southwest China. At present, the main method for obtaining the dynamic response of the layered soil layer is the one-dimensional equivalent linearised wave method [27]. Based on the soil dynamic constitutive model, Jin et al. proposed an explicit finite element method (FEM) for the seismic response of horizontally stratified sites under the condition of transmitting artificial boundaries [28]. According to the propagation principle of seismic waves in layered elastic media, Fan et al. proposed a fast time-history algorithm for calculating the seismic response of layered soil sites by using the method of elastic wave superposition [29]. Fan et al. studied the seismic response of horizontally stratified sites under seismic conditions by using a shaking table test in the time-frequency domain [20]. At present, most of the theoretical calculation methods for the seismic response of horizontally stratified sites are based on the assumption of shear wave incidence at the site base, and most of the calculation methods adopt equivalent linearisation simplification. However, in practice, the seismic response of the site has strong nonlinear characteristics. Therefore, the obtained site dynamic response characteristics based on the shear wave incidence hypothesis and equivalent linearisation simplified calculation need to be further verified.

At present, the dynamic response of sites is commonly based on time domain acceleration response analysis [30–32]. Complex slopes have a significant effect on the dynamic mechanics of the sites and lead to significant changes in the frequency components of waves due to wave refraction and reflection effects near the discontinuities in the rock mass [33,34]. Time domain analysis using PGA (peak ground acceleration) cannot comprehensively reflect the seismic response of sites; therefore, their seismic response should be studied in the frequency domain. The fast Fourier transform (FFT) algorithm is the preferred method for investigating the dynamic response of sites [35,36]. In addition, because seismic waves are nonlinear and unsteady signals, there are few studies on the seismic response of sites based on their own characteristic parameters and physical quantities [37,38]. The Hilbert-Huang transform (HHT) is the preferred method to deal with nonlinear and unsteady signals and has a good time-frequency resolution [39]. However, the previous study of the seismic response of sites paid more attention to the analysis of a single domain, and time-frequency joint domain analysis was ignored. Therefore, to better understand the seismic response of layered sites from all directions and angles, a multidomain analysis method needs to be established.

This work takes layered sites in the southwest Sichuan Basin, China as examples (Figure 1). A multidomain analysis method is used to investigate the seismic response of the layered sites under earthquake excitation (Figure 2). Three generalised geological models of the layered site are as follows: homogeneous site (Model 1), horizontally layered

site (Model 2) and tilted layered site (Model 3). The layered sites contain hard rock, soft rock and gravelly soil (Figure 3). The seismic response characteristics of the layered sites were studied using FEM dynamic analyses according to the acceleration-time histories, modal analysis, Fourier transform, seismic Hilbert energy and marginal spectrum analysis. The wave propagation characteristics through the layered sites and their influence on the seismic response are studied. A new time domain analysis parameter $PGA_{(IMF)}$ based on the empirical mode decomposition (EMD) method is proposed, and its applicability is verified and compared by using PGA. According to the analyses of the time, frequency and time-frequency domains, the dynamic amplification effects of the layered sites are studied. In particular, the influence of the natural frequency of sites on their seismic response characteristics is discussed, and their dynamic response is also analysed from the perspective of energy transmission characteristics.

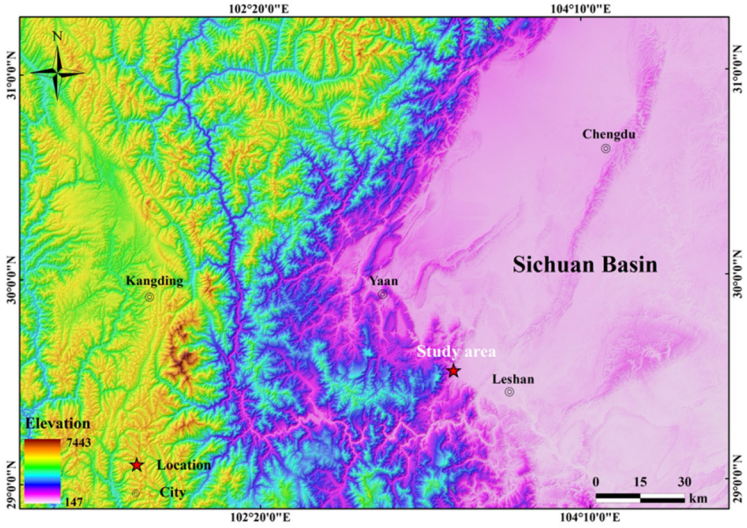


Figure 1. Location of the study area.

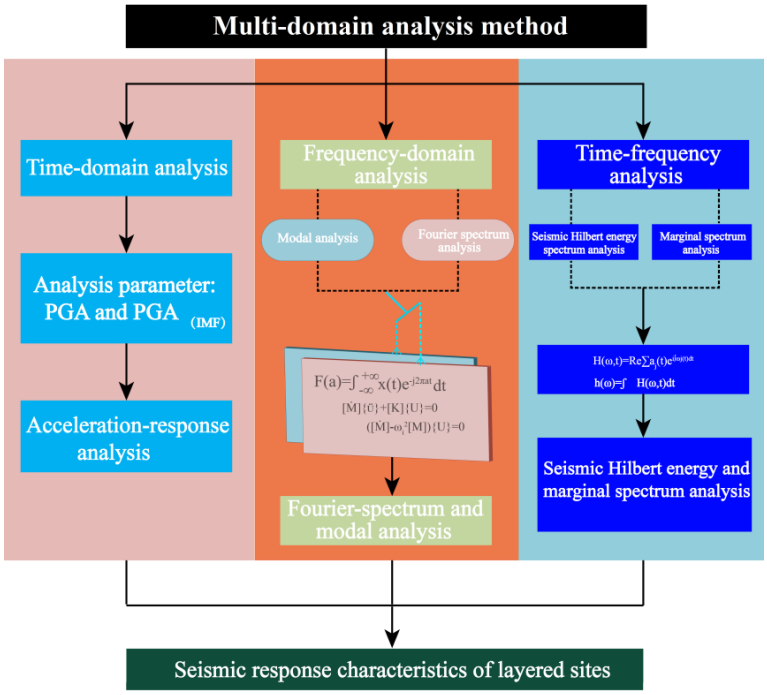


Figure 2. Flowchart for multidomain analysis method.

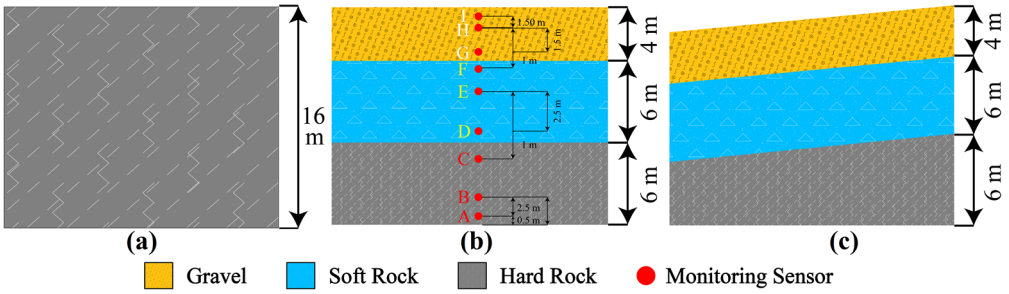


Figure 3. Geological section of the horizontally layered field and layout of the measuring points A-I in the models: (**a**) homogeneous site (Model 1), (**b**) horizontally layered site (Model 2) and (**c**) tilted layered site (Model 3).

2. Methodology

2.1. Time Domain Analysis

The acceleration-time history is the core parameter for analysing the seismic response of rock-soil masses [31,32]. The PGA is selected as the analysis parameter, which reflects the strongest response in the whole acceleration-time history and the maximum seismic inertial force at a certain position in the sites. Based on the previous dynamic response analysis parameters of rock-soil mass, this work proposed using the PGA amplification coefficient of a certain order of intrinsic mode function IMF ($M_{PGA(IMF)}$) as the analysis parameter and performs a comparative analysis with the traditional PGA amplification coefficient (M_{PGA}) of collected signals to discuss the applicability of the two analysis parameters. The $M_{PGA(IMF)}/M_{PGA}$ represents the PGA ratio of a point on the bedrock of the sites, showing the PGA magnification rate. The analysis parameter acquisition method is as follows. First, the original signal is divided into a series of IMFs by the EMD method. Second, channel switching is performed to transform the multichannel signals composed of multiple IMFs into single-channel signals composed of a single IMF. Third, the instantaneous frequency of each IMF is solved, and its time-frequency curve is plotted. Finally, an IMF of a certain order with high instantaneous frequency identification, rich frequency components and large acceleration amplitude is selected as the target IMF, and its $PGA_{(IMF)}$ is adopted as the analysis parameter to study the seismic amplification effect of the layered site.

2.2. Frequency Domain Analysis

Frequency domain analysis includes FFT and finite element modal analysis. Modal analysis can reveal the inherent characteristics of engineering entities, including their natural frequency and vibration mode, which can also predict their dynamic response in the elastic domain. The modal analysis equation is as follows: $[M_0]\{U_0\} + [K]\{U\} = 0$ [40]. The corresponding characteristic equation is as follows: $([M_0]\text{-}\omega_i{}^2[M])\{U\} = 0$. Then, the natural frequency f_i is: $f_i = \omega_i/2\pi$. $\{U\}_i$ is the eigenvalue, which refers to a certain vibration mode of the model. In addition, FFT is used to analyse the vibration responses of rock and soil masses, which can clearly identify different frequency components of a signal. FFT can quickly identify the main components of the signal and can be quickly filtered, and has become a common method for dealing with seismic signals. The essence of FFT is to decompose the seismic signal $a(t)$ into a combination of several sine waves of different frequencies, $F(a)$. The mathematical expression for the FFT is as follows: $F(a) = \int_{-\infty}^{+\infty} x(t)e^{-j2\pi at}dt$, where $a(t)$ is the acceleration time history [41].

2.3. Time-Frequency Domain Analysis

The HHT is a common time-frequency domain analysis method that includes two parts: the EMD method and Hilbert spectrum analysis [38]. The HHT provides an effective and feasible method for identifying seismic Hilbert energy distributions. According to the uses of EMD, any complex dataset is broken down into a finite IMF (Figure 4) [42]. The

Hilbert spectrum, $H(\omega, t)$, is as follows [43,44]: $H(\omega, t) = \mathrm{Re}\sum_{j=1}^{n} a_j(t)e^{i\int \omega_j(t)dt}$. The HHT marginal spectrum, $h(\omega)$, is as follows: $h(\omega) = \int_0^T H(\omega, t)dt$. In the marginal spectrum, by accumulating the energy of each instantaneous frequency, the total energy of the frequency in the original signal can be calculated; that is, the marginal spectrum amplitude. Through the HHT of different IMFs, the corresponding Hilbert spectrum of each IMF is obtained, and then the marginal spectrum of the IMF is obtained by integrating the Hilbert spectrum. The corresponding energy spectrum is obtained by squaring the Hilbert spectrum amplitude of all IMFs, and the total seismic Hilbert energy spectrum of the original seismic wave can be obtained by adding the energy spectrum of all IMFs.

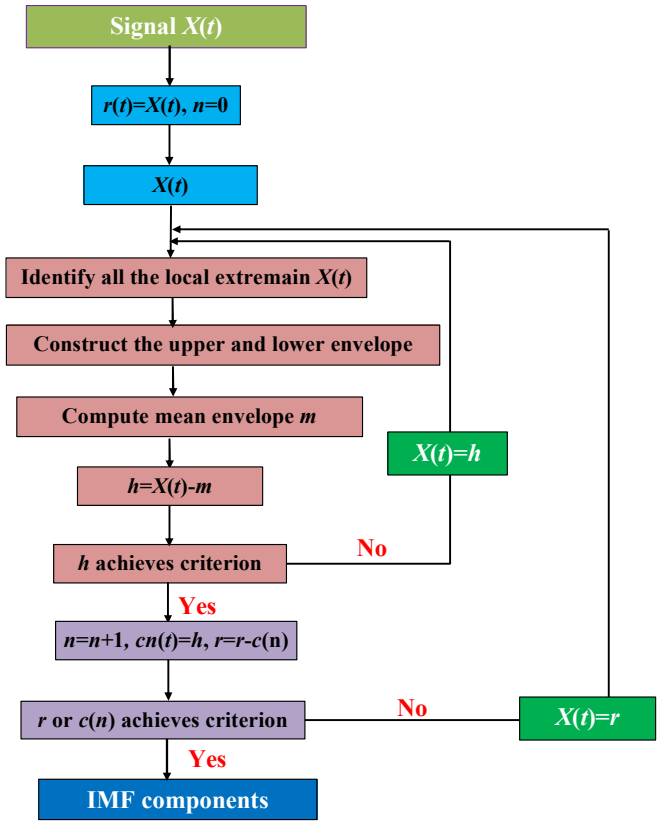


Figure 4. Flowchart for EMD approach [43].

3. Finite Element Model of Layered Sites

Analysis of Wave Propagation Characteristics in the Slope

Abaqus/Explicit and Abaqus/Frequency are used to perform the dynamic analyses and modal analysis. Abaqus/Explicit is used to perform transient dynamic simulations (Abaqus Explicit User Manual). The elastic model and Mohr-Coulomb criterion were used in the FEM simulation. In finite element dynamic analysis, the optimisation of the boundary condition, degree and subdivision size of the model is of great significance for accurately simulating the mechanism of wave propagation in discontinuous media. The connection mode between the different types of rock-soil masses is set to the "nonsurface contact" mode without viscous damping by using the "tie connection" method. When the reflection coefficient between the different types of rock-soil mass contact surfaces is large, multiple wave reflections should be considered. The main influence of the different types of rock-soil mass contact surfaces on the incident wave propagation is the deceleration and attenuation of the incident wave. The boundary conditions are a key influencing factor in the dynamic analysis of rock mass sites [45–48]. The actual foundation of a site is infinite; hence, the infinite element boundary method was adopted in the model, and

infinite element boundary conditions were adopted on both sides and on the bottom of the models. The infinite element boundary was used to absorb the radiation energy of waves, and the adverse effects of the reflected waves were weakened in the dynamic analysis.

Three FEM models for the layered sites were modelled. The model size was 20,000 × 16,000 mm (Figure 5). The calculation of the in situ stress balance was carried out first, before the numerical simulation. The infinite element boundary included 290 infinite elements. A total of 12,360 elements and 13,584 grid modes were generated in the rock mass. The material parameters of the layered sites are listed in Table 1. A schematic diagram of the boundary conditions of the numerical model is shown in Figure 6. To simulate the influence of seismic waves on the dynamic response of the layered sites, the Wenchuan earthquake (WE) wave (0.08 g) recorded by the Wudu earthquake station, China, was loaded at the bottom of the models (Figure 7). The dominant frequency of the WE wave was approximately 7.7 Hz, t = 120 s and Δt = 0.005 s. Ground motion was simulated by inputting waves at the interface between finite elements and infinite elements at the bottom of the model.

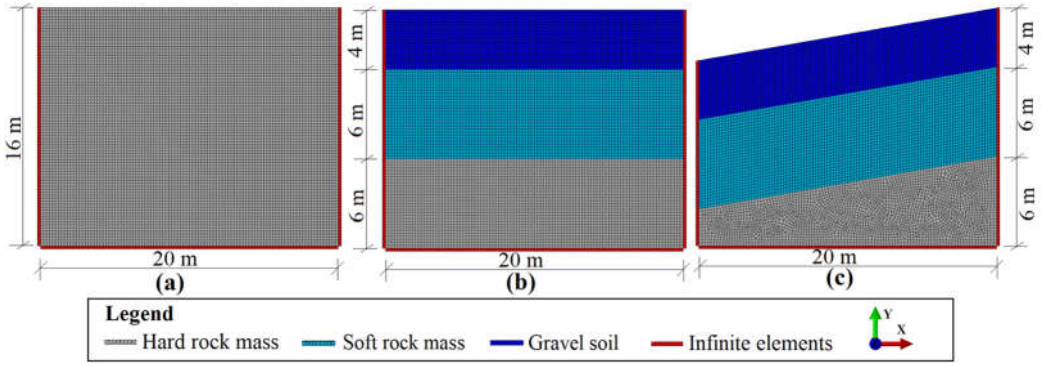


Figure 5. Mesh model used in the calculations: (**a**) homogeneous rock mass site (Model 1), (**b**) horizontally layered site (Model 2) and (**c**) layered site with strata dip angle of 10° (Model 3).

Table 1. Physico-mechanical parameters of the material parameters of the sites [9,20].

Physical and Mechanical Parameters	Density ρ (kg/m^3)	Poisson Ratio μ	Dynamic Elastic Modulus E/MPa	Friction Angle φ (°)	Cohesive Force c (kPa)
Hard rock	2300	0.16	2100	45	2000
Soft rock	2200	0.2	2780	41	1040
Gravel soil	1990	0.25	1.5	25	180

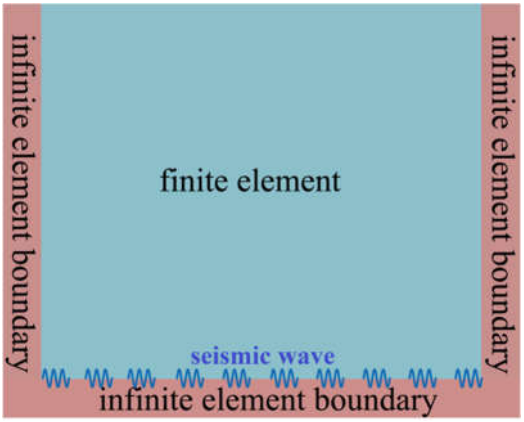


Figure 6. Schematic diagram of the boundary conditions of the numerical model.

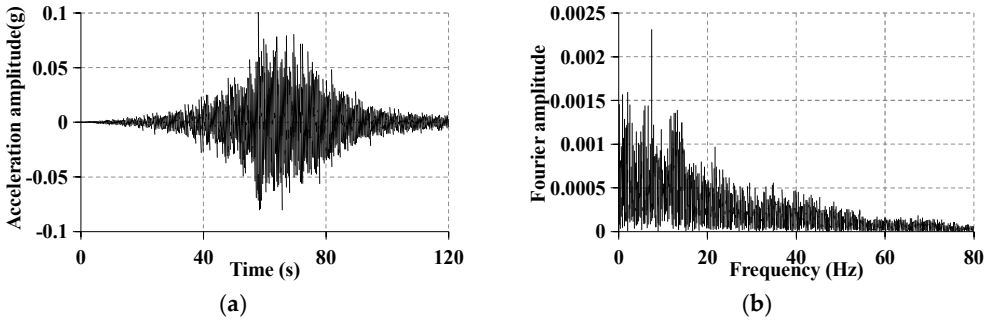


Figure 7. The input WE wave (0.08 g): (**a**) Time history, (**b**) Fourier spectrum.

4. Seismic Response Characteristics of Layered Sites

4.1. Results of Time Domain Analysis

4.1.1. Wave Propagation Characteristics in Layered Sites

To investigate the seismic wave propagation characteristics at layered sites, Models 1 and 2 are taken as examples, with their acceleration distribution characteristics shown in Figure 8. Figure 8a shows that when waves propagate in homogeneous rock sites, the acceleration shows a layered amplification effect; that is, seismic waves show obvious layered propagation characteristics. Figure 8b shows that the seismic wave propagation characteristics are relatively complex in the horizontally layered site, and the acceleration in the layered site shows a local amplification effect; in particular, the acceleration near the rock mass interface exhibits an obvious phase shift. Compared with Model 1, the wave propagation characteristics of Model 2 are more complex. This is because Model 2 contains three kinds of rock and soil bodies, and there will be multiple phenomena of seismic wave reflection and refraction near the interface of different rock and gravel soils, resulting in seismic wave superposition or weakening and leading to a magnified or reduced local acceleration effect at the layered site. Figure 8b shows that the dynamic amplification effect of waves mainly appears in the gravel soil layer (ground surface area). The gravel soil layer has a great influence on the seismic wave propagation characteristics at the layered sites.

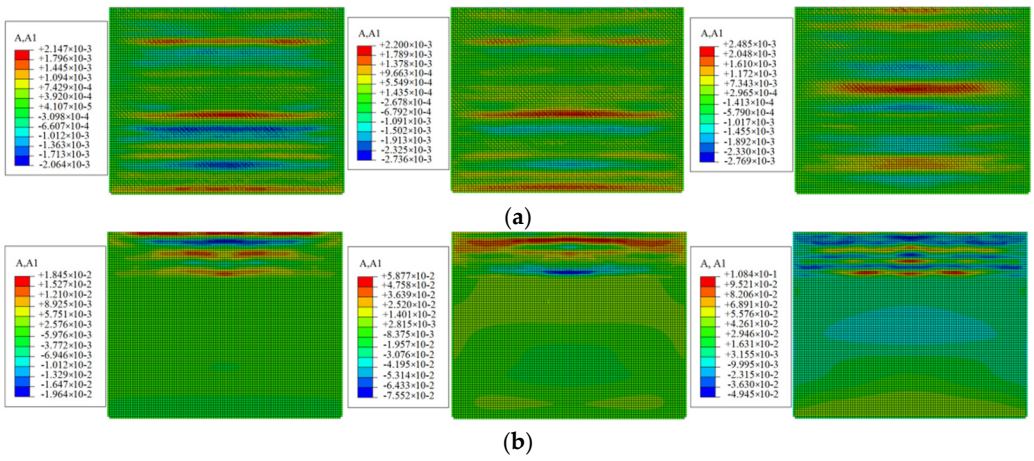


Figure 8. Acceleration distribution during wave propagation in Model 1 when the WE wave is input in the *x* direction: (**a**) Model 1 (t = 1.80 s; t = 1.95 s; t = 2.05 s), (**b**) Model 2 (t = 1.95 s; t = 2.15 s; t = 2.30 s). (Unit: m/s^2).

4.1.2. Dynamic Response Characteristics of Layered Sites

To study the dynamic amplification effect of the layered sites, the time history curves of waves were extracted from the measuring points in the models, and their dynamic response characteristics were studied by analysing the PGA. For many measurement points in the models, typical measurement points in Model 2 are taken as examples (Figure 3b).

Their acceleration-time history and their corresponding Fourier spectra are shown in Figure 9. The PGA in Model 2 increases with elevation, which indicates that elevation has an obvious magnification effect. In addition, the input seismic wave is a WE wave, whose waveform and frequency components are very complex when propagating in layered sites; hence, a new analysis parameter of PGA is proposed. The seismic signals collected were decomposed by the EMD method to obtain a series of IMFs, and the PGA of the IMF with a certain high resolution was selected as the parameter to analyse the dynamic amplification effect of the layered site (Figure 10a). The IMF has local transient characteristics, which can better reflect the characteristics of the original signal.

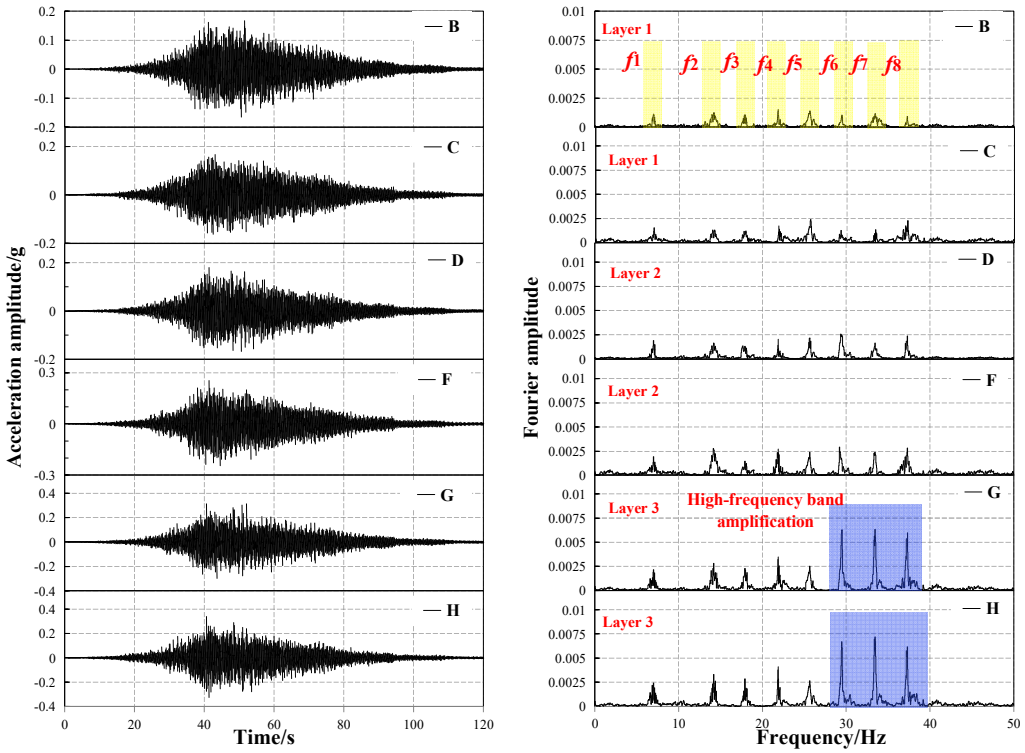


Figure 9. Seismic response of typical points (B, C, D, F, G, and H) at the surface of Model 2 when inputting the WE wave in the *x* direction: (**a**) acceleration-time history, (**b**) Fourier spectrum.

The dynamic response of the layered sites was analysed by comparing the $MPGA_{(IMF)}$ and M_{PGA}. The $M_{PGA(IMF)}$ and M_{PGA} refer to the ratio of $PGA/PGA_{(IMF)}$ of a certain point to point A at the bottom of the models. Taking the input 0.08 g horizontal WE wave as an example, IMFs and their instantaneous frequency curves can be obtained after EMD of the WE wave (Figure 10). The first six IMFs can contain the information of the original signal. IMF2 has the largest amplitude, and its frequency components in the instantaneous frequency curve are rich and easy to identify. Therefore, IMF2 is selected to obtain the $M_{PGA(IMF)}$, earthquake Hilbert energy and marginal spectrum.

The PGAs and their magnification coefficients of the models are shown in Table 2 and Figures 11 and 12. The M_{PGA} and $M_{PGA(IMF)}$ of the models increased with elevation, indicating that there was a significant elevation dynamic amplification effect in layered sites under earthquake excitation. Figures 11 and 12 show that the sequences of the M_{PGA} and $M_{PGA(IMF)}$ of the models are as follows: Model 1 < Model 2 < Model 3. This suggests that the seismic magnification effect of the horizontally layered site is greater than that of the homogeneous site and that that of the tilted layered site is the largest; that is, the stratum angle has an influence on the seismic amplification effect of the layered sites.

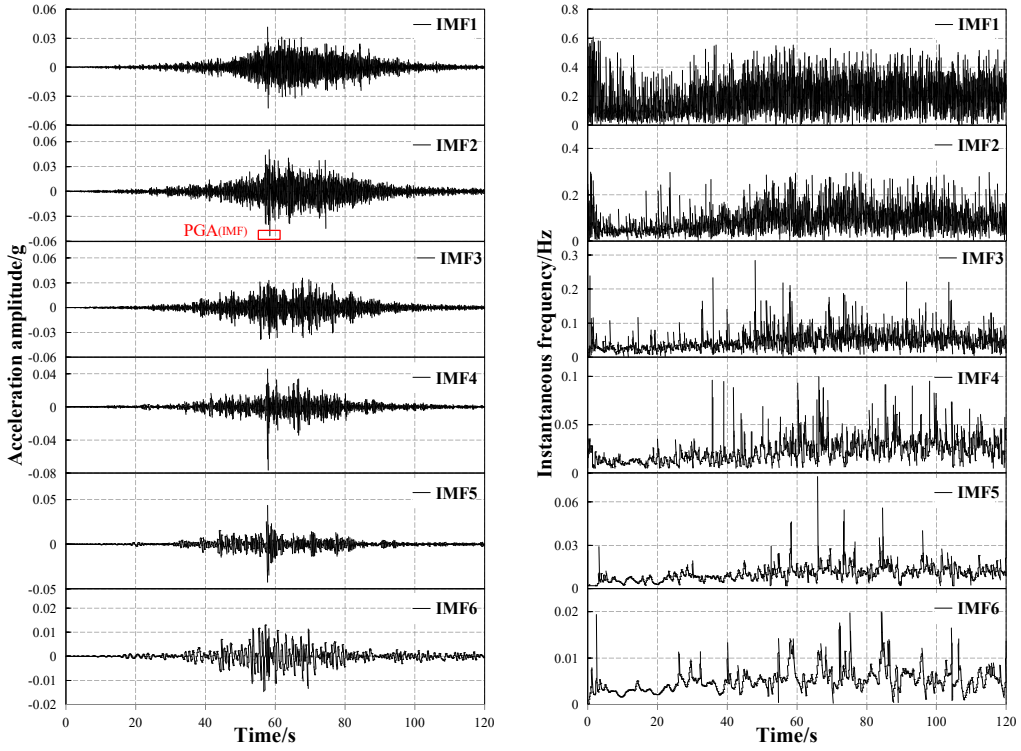


Figure 10. EMD results of the input WE wave (0.08 g): (**a**) IMFs 1–6, (**b**) the corresponding instantaneous frequencies of the IMFs.

Table 2. The PGA of the models when the WE wave was input in the *x* direction (0.08 g).

Elevation/m	Measuring Points	PGA/g		
		Model 1	Model 2	Model 3
0.5	A	0.095	0.103	0.113
3	B	0.101	0.121	0.131
5.5	C	0.106	0.132	0.145
6.5	D	0.115	0.139	0.154
9	E	0.128	0.154	0.164
11.5	F	0.137	0.164	0.183
12.5	G	0.148	0.184	0.198
14	H	0.161	0.228	0.241
15.5	I	0.170	0.231	0.247

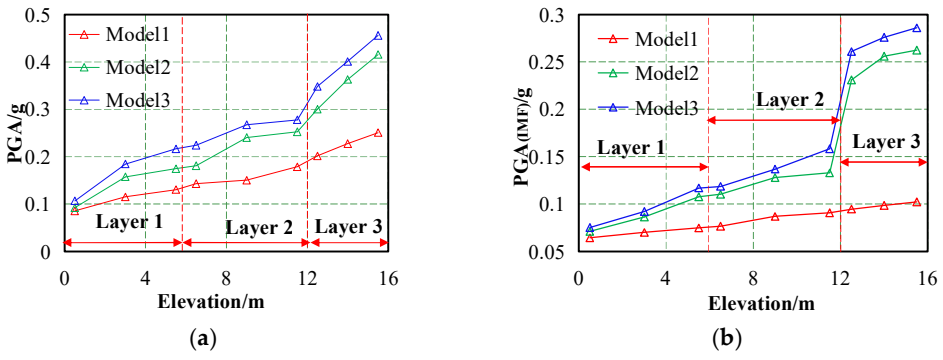


Figure 11. Change in PGA of the models when input in the *x*-direction: (**a**) PGA, (**b**) $PGA_{(IMF)}$.

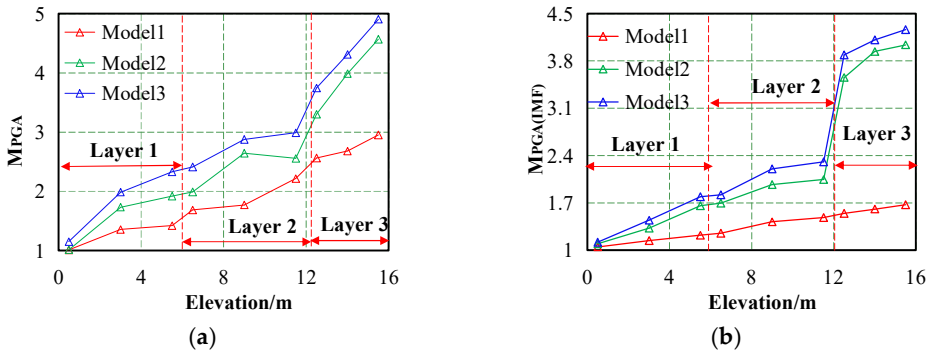


Figure 12. Change of the PGA amplification coefficient of the models when inputting the WE wave in the *x* direction: (**a**) M_{PGA} and (**b**) $M_{PGA(IMF)}$.

Compared with PGA/M_{PGA}, $PGA_{(IMF)}/M_{PGA(IMF)}$ can be used to further analyse the influence of different strata on the site dynamic amplification effect. Figures 11b and 12b show that there is little difference in $PGA_{(IMF)}$ and $M_{PGA(IMF)}$ on both sides of the interface between Layers 1 and 2, which indicates that there is little difference in dynamic response characteristics between hard rock and soft rock in the layered site, and that the dynamic amplification effect of the interface between soft rock and hard rock is relatively small. Figures 11b and 12b show that, compared with Model 1, $PGA_{(IMF)}$ and $M_{PGA(IMF)}$ on both sides of the interface between Layers 2 (soft rock) and 3 (gravel soil) are significantly different, showing a rapid increase from soft rock to gravel soil. This is because Model 1 is a homogeneous hard rock site, but Models 2 and 3 are layered sites, whose topmost layer is gravel soil. This shows that, compared with the rock mass site, the overlying gravel soil has an obvious dynamic amplification effect at the sites. Moreover, Figure 12a shows that the dynamic magnification effect of the horizontally layered site using FEM dynamic analyses is consistent with that using shaking table tests [20,23], which indicates that the numerical results in this work are reliable.

Given the analysis mentioned above, compared with PGA, $PGA_{(IMF)}$ can better reflect the influence of different strata on the seismic response of the sites. PGA and $PGA_{(IMF)}$ have their own advantages. PGA more easily and directly obtainable, while $PGA_{(IMF)}$ is more complex, requiring decomposition by the EMD method and further selection. Therefore, $PGA_{(IMF)}$ can be considered an important seismic amplification effect analysis parameter in future studies and can be used as a verification supplement of PGA analysis results to make the seismic dynamic response characteristic analysis results more reliable.

4.2. Results of Frequency Domain Analysis

4.2.1. Modal Analysis

The vibration modes and natural frequencies of the models using modal analysis are shown in Table 3 and Figure 13. The natural frequency of Model 1 is larger than that of Model 2, and that of Model 3 is the smallest (Table 3). The first-order mode is the main vibration mode of models, which can reflect their main dynamic deformation characteristics. Figure 13 shows that the relative displacement U_{max} mainly occurs in the surface area, which shows that the dynamic magnification effect of the models is mainly located in the ground surface area. Compared with Model 1, the first-order vibration mode of Models 2 and 3 shows that U_{max} is mainly concentrated in the gravel soil layer. This is because Models 2 and 3 are layered sites, and the difference in strata leads to the change in the dynamic deformation characteristics of the sites. Figure 13b,c shows that the first-order modes mainly show the overall deformation of gravel soil, while the second- and third-order modes indicate the local deformation of gravel soil. This indicates that the low-order natural frequency primarily causes the large-scale overall deformation of the site's ground surface, while the high-order natural frequency primarily causes the local deformation of the site.

Table 3. The predominant frequency and modal analysis results of Model 2.

Fourier Spectrum Analysis		Modal Analysis	
Predominant Frequency	**Value/Hz**	**Order**	**Natural Frequency/Hz**
f_1	7–8	1	7.05
f_2	14–15	2	14.56
f_3	17–18	3	18.12
f_4	21–22	4	22.16
f_5	25–26	5	25.97
f_6	29–30	6	29.46
f_7	33–34	7	33.45
f_8	37–38	8	37.38

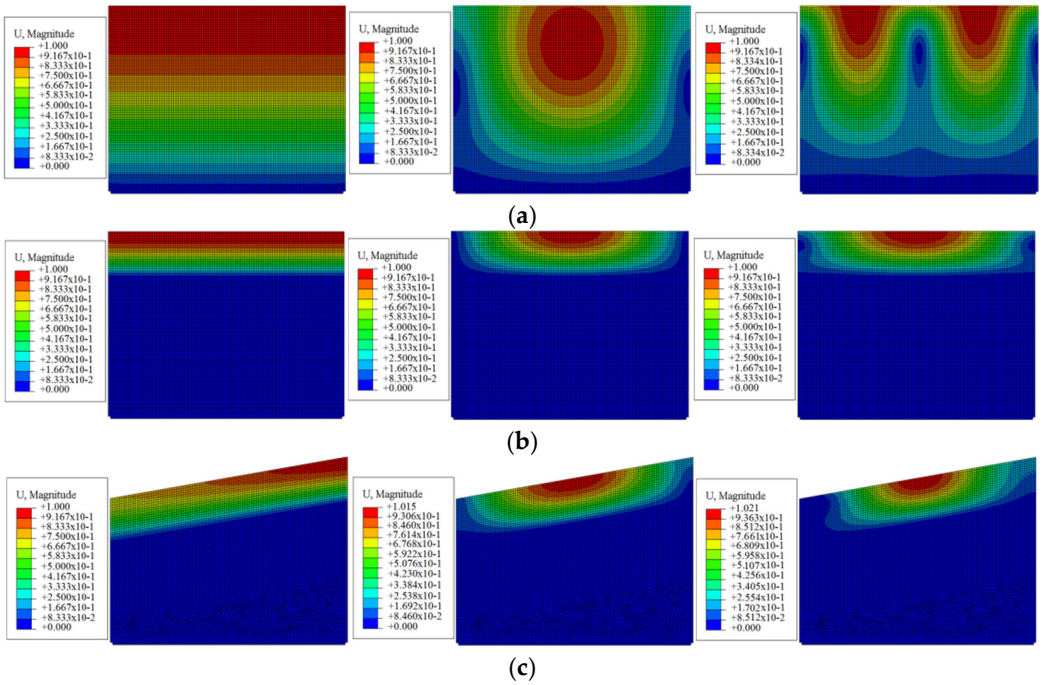


Figure 13. First three vibration modes of the models: (**a**) Model 1, (**b**) Model 2, (**c**) Model 3. Modes 1–3 are shown from left to the right.

4.2.2. Fourier Spectrum Analysis

Taking Model 2 as an example, two measurement points for each layer were selected and their Fourier spectra are shown in Figure 9b. Figure 9b shows that the predominant frequency of the horizontally layered site is mainly concentrated in the range of 40 Hz, and eight predominant frequencies (f_1–f_8) can be clearly found within 0–40 Hz (Table 3). The PFSA (peak Fourier spectrum amplitude) of f_1–f_8 changes with elevation and is shown in Figure 14. Figures 9b and 14 show that in Layers 1 and 2 (hard and soft rock layers), the PFSA of different natural frequency bands of measuring points (B, C, D and F) increases to a certain extent with elevation. This indicates that soft and hard rock mass strata have little influence on the Fourier spectrum characteristics and that the spectral peak value mainly increases to a certain extent. Compared with the hard and soft rock strata, the PFSA of f_1–f_5 at measuring points G and H in the third layer (gravel soil layer) increased to a certain extent; in particular, the PFSA of f_6–f_8 was rapidly amplified from Layer 2 to 3. This indicates that overlying gravel soil has an obvious amplifying effect on the high-frequency spectrum amplitude, which is consistent with the results of modal analysis (Figure 13), and the high-order natural frequency mainly induces local deformation of the gravel soil stratum. In addition, Table 3 shows that the natural frequencies obtained by Fourier spectrum analysis and modal analysis are consistent, which indicates that the first

eight natural frequencies of Model 2 can be determined based on Fourier spectrum analysis and modal analysis.

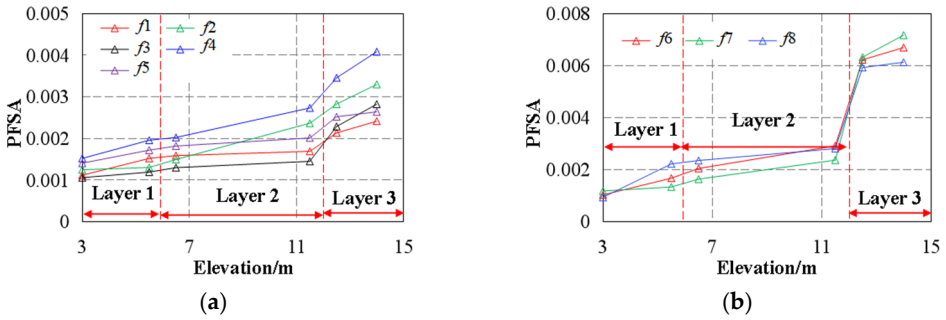


Figure 14. Change of the PFSA in Model 2 when inputting the WE wave in the x direction at different natural frequencies: (**a**) f_1–f_5 and (**b**) f_6–f_8.

4.3. Results of Time-Frequency Domain Analysis

The propagation characteristics of seismic energy in the time-frequency domain can be studied by analysing the variation of seismic Hilbert energy spectrum characteristics and the amplitude of seismic waves. The seismic response characteristics of layered sites can be further studied from the perspective of energy. The HHT is used to clarify the influence of (1) the interface between the soft rock mass and gravel soil and (2) the interface between the soft and hard rock masses on the change in wave energy in the layered sites. The latter is also used to study the change in wave energy during the wave propagation process in the surface gravel soil.

Taking points A–I of the three strata in Model 2 as examples, according to the analyses of their Hilbert energy spectra (Figure 15), the seismic Hilbert energy of the horizontally layered site is mainly distributed within 24–25 s and 7–13 Hz. It should be noted that the PHSA (peak Hilbert energy spectrum amplitude) is within 9–10 Hz, suggesting that the low-frequency band has a great influence on the seismic response of the horizontally layered site. Figure 15a shows that in the hard rock, the Hilbert energy spectrum of points A–C shows single peak characteristics, the spectrum amplitude near the PHSA is small, and the frequency component is not rich. When waves are transferred from Layers 1 (hard rock) to 2 (soft rock), the Hilbert energy spectrum characteristics near the interface between soft and hard rock masses show obvious changes. Figure 15b shows that the influence of the interface between Layers 1 (hard rock) and 2 (soft rock) on the wave energy transmission is mainly manifested as the change in frequency components near the PHSA. As waves pass through the stratigraphic interface, the frequency components around the PHSA become more abundant, from a single peak to multiple peaks, but the PHSA and its occurrence time and frequency are not basically changed. This is because refraction and reflection effects of waves occur near the soft rock/hard rock stratum interface due to lithology changes, leading to frequency components becoming abundant near the PHSA. In addition, to investigate the change in energy when waves propagate from bottom to top in the weak gravelly soil layer, the Hilbert energy spectrum of points G–I is shown in Figure 15c. When the wave enters Layer 2 (soft rock) from Layer 3 (gravelly soil), the shape and peak value of the energy spectrum above the interface between gravelly soil and soft rock change greatly. Compared with Layer 2, the PHSA of the seismic wave is significantly magnified from the bottom to the top of the gravelly soil layer, and the multipeak characteristics of the energy spectrum are more obvious. The frequency components near the PHSA of seismic waves become more abundant, and the energy spectrum amplitude near the PHSA shows a significant amplification effect. The amplitude of the Hilbert energy spectrum in the high-frequency band (28–36 Hz) showed an obvious amplification effect, but the appearance location of the seismic Hilbert energy peak had no basic change. This phenomenon suggests that the interface between gravel soil and soft rock magnifies the peak energy of seismic waves, but

the interface has no effect on the appearance location of the PHSA of seismic waves. When waves propagate in the gravel soil layer, the energy spectrum amplitude of the peak value and its vicinity is significantly amplified, especially in the high-frequency band (f_6–f_8). This indicates that the horizontally layered site can be analysed from the perspective of high-frequency components. Compared with the soft rock, the characteristics of the Hilbert energy spectrum in gravelly soil are changed for the following reasons: gravelly soil is a multiphase medium, and the propagation of seismic waves in multiple media changes the characteristics of seismic energy transmission; compared with hard and soft rocks, gravelly soil has fewer constraints; meanwhile, as the surface is a free surface, the superposition effect of seismic waves appears near the ground surface, resulting in a greater displacement response of the top gravelly soil and changes in the shape of the Hilbert energy spectrum.

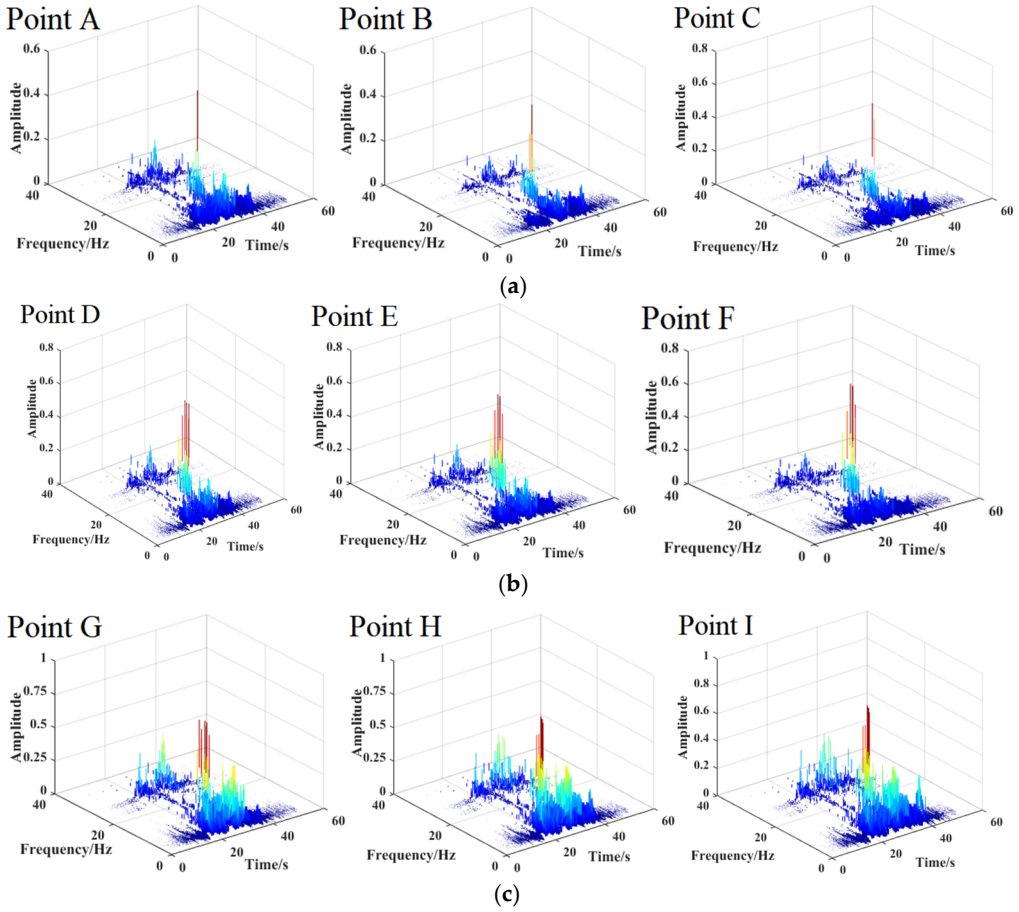


Figure 15. Seismic Hilbert energy spectrum of different strata of Model 2: (**a**) layer 1, (**b**) layer 2, (**c**) layer 3.

In addition, taking measuring points (B, E, H, and I) of Model 2 as examples, their marginal spectra are shown in Figure 16. After EMD decomposition of the original seismic wave signal, IMF of a certain order with high resolution was selected, and HHT was applied to obtain the marginal spectrum. Figure 16 shows that the PMSA (peak marginal spectrum amplitude) primarily occurs in the high-frequency band (28–35 Hz), and the position of the PMSA is consistent with that of the Hilbert energy spectrum. Figure 16 shows that from the bedrock to the gravel soil, the high-frequency components of the marginal spectrum of waves are more abundant, and the amplitude is gradually amplified; meanwhile, the range of the marginal spectrum energy concentration segment also increases. Figure 16 shows that from Layer 1 (hard rock) to 2 (soft rock), the spectral features of the marginal spectrum change little and mainly manifest as an increase in the spectral amplitude. Figure 16 shows that from Layer 2 (soft rock) entering Layer 3 (gravel soil), the frequency components of the

marginal spectrum became more abundant, and the spectral peak increased significantly, indicating that gravel soil had an obvious amplification effect on seismic energy transmission, which was consistent with the analysis of the seismic Hilbert energy spectrum. Moreover, to further analyse the dynamic amplification effect of strata on the layered sites from the perspective of energy, the PHSA and PMSA (peak marginal spectrum amplitude) of the three models increased with elevation, as shown in Figure 17. The PHSA and PMSA of Model 1 show a linear increasing trend with elevation. In Models 2 and 3, PHSA and PMSA increase sharply when the soft rock enters the gravel soil, which indicates that the gravel soil has an obvious amplification effect on the seismic wave energy.

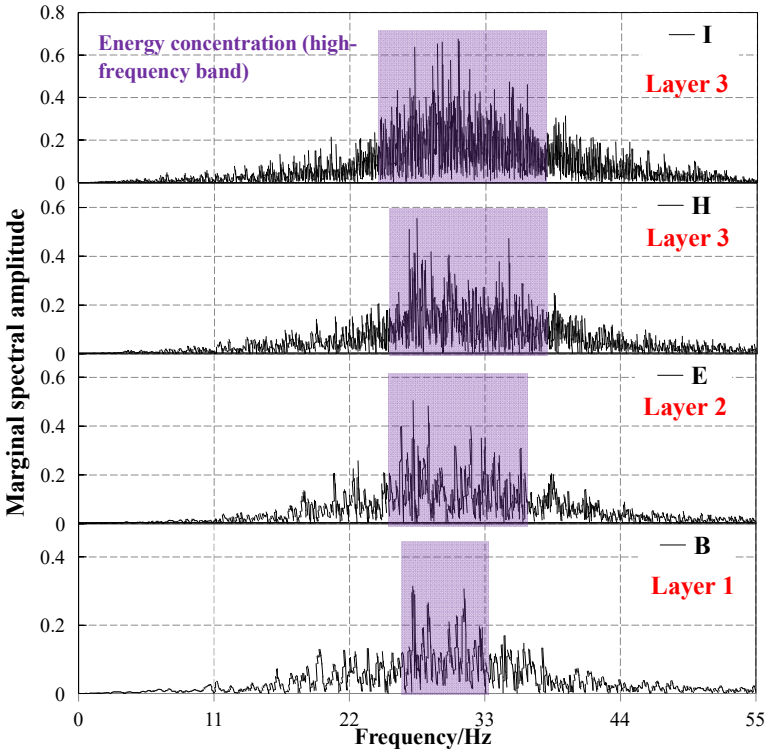


Figure 16. The marginal spectrum of different measuring points (I, H, E, and B) of Model 2.

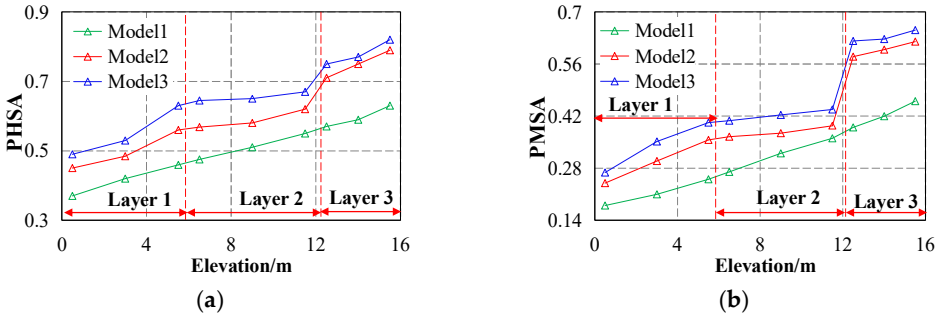


Figure 17. Change of PMSA and PHSA with increasing elevation: (**a**) PMSA and (**b**) PHSA.

5. Conclusions

The seismic response of layered sites was investigated based on multidomain analysis. Some main conclusions are as follows.

(1) According to the multidomain analysis, elevation and stratum properties have a magnification effect on the seismic response of the layered sites. The PGA, PFSA, PHSA and PMSA increase gradually with elevation at the layered sites. The characteristics of wave propagation at layered sites are complex, and a weak gravel soil layer has a great influence on the seismic wave propagation characteristics. The dynamic

amplification effect of the interface between soft rock and hard rock is relatively small, while overlying gravel soil has a greater amplification effect on seismic waves than rock mass. The seismic amplification effect of the models is as follows: Model 3 > Model 2 > Model 1. $PGA_{(IMF)}$ was proposed to analyse the dynamic amplification effect of layered sites, which can better reflect the influence of different strata on their seismic response characteristics.

(2) The natural frequencies of the layered sites can be determined using Fourier spectrum and modal analysis. Natural frequencies have a significant influence on the dynamic deformation response of the sites. Frequency domain analysis shows that the interface of soft and hard rock mass strata has little influence on the Fourier spectrum characteristics of the sites, and only the PFSA mainly increases to a certain extent. The overlying gravel soil has an obvious magnification effect on the PFSA and U; in our study, the PFSA of the high-frequency band of seismic waves was greatly amplified, and the PFSA of f_6–f_8 ($\geq$30 Hz) in the gravel soil layer increased rapidly.

(3) The seismic energy in the Hilbert energy spectrum and marginal spectrum of the horizontally layered site is mainly distributed in low-order natural frequencies (7–13 Hz) and high-order natural frequencies (27–34 Hz), respectively. Stratum properties have a significant effect on the Hilbert energy spectrum characteristics in layered sites. When waves pass from hard rock to soft rock, the peak value of the seismic Hilbert energy spectrum changes from single to multiple peaks, and the frequency components near the peak become more abundant. When the seismic wave enters gravelly soil, the Hilbert energy spectral peak and its nearby amplitude are significantly magnified, and the frequency components near the PHSA become more abundant. In our study, the seismic energy of the Hilbert energy spectrum in the high-frequency band (28–36 Hz) was obviously amplified. Moreover, the marginal spectrum characteristics changed with elevation in the layered sites. Compared with hard/soft rock, gravel soil had an obvious amplification effect on seismic energy transmission. The PMSA increased with elevation in the high-frequency band; in particular, the frequency components and spectral amplitude of the marginal spectrum became more abundant and significantly larger in gravelly soil.

Author Contributions: Methodology, D.S.; Writing—original draft, L.D. and G.L.; Writing—review & editing, D.S. and G.L. All authors have read and agreed to the published version of the manuscript.

Funding: The National Natural Science Foundation of China (52090081, 41941019, 52109125), the China Postdoctoral Science Foundation (2020M680583), the National Postdoctoral Program for Innovative Talent of China (BX20200191), the Excellent Sino-foreign Youth Exchange Program of China Association for Science and Technology in 2020 (No. 58), and the Shuimu Tsinghua Scholar Program (2019SM058).

Institutional Review Board Statement: Not applicable.

Informed Consent Statement: Not applicable.

Data Availability Statement: The data used to support the findings of this study are available from the corresponding author upon request.

Acknowledgments: The authors would like to thank the editor and the reviewers for their contributions.

Conflicts of Interest: The authors declare that they have no conflict of interest.

References

1. Yin, Y.; Li, B.; Wang, W. Dynamic analysis of the stabilized Wangjiayan landslide in the Wenchuan Ms 8.0 earthquake and aftershocks. *Landslides* **2015**, *12*, 537–547. [CrossRef]
2. Dai, F.; Xu, C.; Yao, X.; Xu, L.; Tu, X.; Gong, Q. Spatial distribution of landslides triggered by the 2008 Ms 8.0 Wenchuan earthquake, China. *J. Asian Earth Sci.* **2011**, *40*, 883–895. [CrossRef]
3. Furuya, M.; Yasuda, T. The 2008 yutian normal faulting earthquake (mw 7.1), nw tibet: Non-planar fault modeling and implications for the karakax fault. *Tectonophysics* **2011**, *511*, 125–133. [CrossRef]

4. Huang, M.W.; Chen, C.Y.; Wu, T.H.; Chang, C.L.; Liu, S.Y.; Kao, C.Y. GIS-based evaluation on the fault motion-induced coseismic landslides. *J. Mt. Sci.* **2012**, *9*, 601–612. [CrossRef]
5. Xu, C.; Xu, X.; Dai, F.; Saraf, A.K. Comparison of different models for susceptibility mapping of earthquake triggered landslides related with the 2008 Wenchuan earthquake in China. *Comput. Geosci.* **2012**, *46*, 317–329. [CrossRef]
6. Li, X.; He, S. Seismically induced slope instabilities and the corresponding treatments: The case of a road in the Wenchuan earthquake hit region. *J. Mt. Sci.* **2009**, *6*, 96–100. [CrossRef]
7. Xu, Q.; Li, Y.R.; Zhang, S.; Dong, X.J. Classification of large-scale landslides induced by the 2008 Wenchuan earthquake, China. *Environ. Earth Sci.* **2016**, *75*, 1–12. [CrossRef]
8. Wang, Z.M.; Zhang, J.J.; Zhang, M.; Tong, X.H. Study on dynamic characteristics of layered site under far field earthquake by shaking table tests. *Constr. Technol.* **2017**, *46*, 110–113.
9. Tang, Y.L.; Yang, C.W. Time-frequency analysis method of seismic responses of the horizontal layer field subjected to shear wave. *Earthq. Eng. Eng. Dyn.* **2016**, *36*, 133–141.
10. Sanz Pérez, E.; Menéndez-Pidal, I.; Galindo Aires, R.; López-Querol, S.; Pascual-Arribas, C. Historical earthquake parameters by geological and seismic site analysis: The 1908 Cerbón earthquake (Spain). *Bull. Eng. Geol. Environ.* **2016**, *75*, 1251–1271. [CrossRef]
11. Song, D.Q.; Chen, J.; Cai, J. Deformation monitoring of rock slope with weak bedding structural plane subject to tunnel excavation. *Arab. J. Geosci.* **2018**, *11*, 251. [CrossRef]
12. Chen, Z.; Song, D.Q.; Hu, C.; Ke, Y.T. The September 16, 2017, Linjiabang landslide in Wanyuan County, China: Preliminary investigation and emergency mitigation. *Landslides* **2020**, *17*, 191–204. [CrossRef]
13. Du, H.; Song, D.Q.; Chen, Z.; Shu, H.; Guo, Z. Prediction model oriented for landslide displacement with step-like curve by applying ensemble empirical mode decomposition and the PSO-ELM method. *J. Clean. Prod.* **2020**, *270*, 122248. [CrossRef]
14. Yu, Y.; Wang, E.Z.; Zhong, J.W.; Liu, X.L.; Li, P.H.; Shi, M.; Zhang, Z.G. Stability analysis of abutment slopes based on long-term monitoring and numerical simulation. *Eng. Geol.* **2014**, *183*, 159–169. [CrossRef]
15. Liu, X.; Han, G.; Wang, E.; Wang, S.; Nawnit, K. Multiscale hierarchical analysis of rock mass and prediction of its mechanical and hydraulic properties. *J. Rock Mech. Geotech. Eng.* **2018**, *10*, 694–702. [CrossRef]
16. Song, D.Q.; Chen, Z.; Hu, C.; Ke, T.; Nie, W. Numerical study on seismic response of a rock slope with discontinuities based on the multi-domain coupled analysis method. *Soil Dyn. Earthq. Eng.* **2020**, *133*, 106112. [CrossRef]
17. Song, D.Q.; Chen, Z.; Ke, Y.; Nie, W. Seismic response analysis of a bedding rock slope based on the multi-domain coupled analysis method: A case study from the middle reach of the Jinsha River, China. *Eng. Geol.* **2020**, *274*, 105731. [CrossRef]
18. Ying, Y.H.; Hu, J.C.; Chen, Q.; Wang, Z.G.; Tsai, M.C. A Blind Thrust and Overlying Folding Earthquake of the 2016 Mw 6.0 Hutubi Earthquake in the Northern Tien Shan Fold-and-Thrust Belts, China. *Bull. Seismol. Soc. Am.* **2019**, *109*, 770–779. [CrossRef]
19. Song, D.Q.; Chen, Z.; Dong, L.H.; Zhu, W. Investigation of the seismic response characteristics of a rock mass slope containing weak structural planes under seismic excitation based on multi-domain coupling analysis. *Geomat. Nat. Hazards Risk* **2021**, *12*, 2776–2802. [CrossRef]
20. Fan, G.; Zhang, J.J.; Zhou, L.R.; Wang, Z.J.; Fu, X. Seismic response of horizontal layered site. *J. Southwest Jiaotong Univ.* **2016**, *51*, 1121–1130.
21. Song, D.; Liu, X.; Li, B.; Zhang, J.; Bastos, J. Assessing the influence of a rapid water drawdown on the seismic response characteristics of a reservoir rock slope using time-frequency analysis. *Acta Geotech.* **2021**, *16*, 1281–1302. [CrossRef]
22. Barker, T.B.; Chen, B.N.; Hague, P.F.; Majain, J.; Wong, K.L. Understanding the time-lapse seismic response of a compacting carbonate field, Offshore Sarawak, Malaysia. *Soc. Pet. Eng.* **2008**, 1853–1866.
23. Song, D.; Liu, X.; Huang, J.; Zhang, J. Energy-based analysis of seismic failure mechanism of a rock slope with discontinuities using Hilbert-Huang transform and marginal spectrum in the time-frequency domain. *Landslides* **2021**, *18*, 105–123. [CrossRef]
24. Celebi, M. Topographical and geological amplification: Case studies and engineering implications. *Struct. Saf.* **1991**, *10*, 199–217. [CrossRef]
25. Bonilla, L.F. Site amplification in the San Fernando valley California: Variability of site-effect estimation using the s-wave coda and h/v methods. *Bull. Seismol. Soc. Am.* **1997**, *87*, 710–730. [CrossRef]
26. Tsuda, K.; Koketsu, K.; Hisada, Y.; Hayakawa, T. Inversion analysis of site responses in the kanto basin using data from a dense strong motion seismograph array. *Bull. Seismol. Soc. Am.* **2010**, *100*, 1276–1287. [CrossRef]
27. Lou, M.L.; Li, Y.C.; Li, N.S.; Wen, F. Some problems in seismic response analysis of soil layer with deep deposit. *J. Tongji Univ.* **2006**, *34*, 427–432.
28. Jin, X.; Kong, G.; Ding, H.P. Nonlinear seismic response analysis of horizontal layered site. *Earthq. Eng. Eng. Vib.* **2004**, *24*, 38–43.
29. Song, D.Q.; Liu, X.L.; Chen, Z.; Chen, J.D.; Cai, J.H. Influence of tunnel excavation on the stability of a bedded rock slope: A case study on the mountainous area in southern Anhui, China. *KSCE J. Civ. Eng.* **2021**, *25*, 114–123. [CrossRef]
30. Lin, Y.; Leng, W.; Yang, G.; Li, L.; Yang, J.S. Seismic response of embankment slopes with different reinforcing measures in shaking table tests. *Nat. Hazards* **2015**, *76*, 791–810. [CrossRef]
31. Song, D.; Liu, X.; Huang, J.; Zhang, Y.; Nkwenti, B.N. Seismic cumulative failure effects on a reservoir bank slope with a complex geological structure considering plastic deformation characteristics using shaking table tests. *Eng. Geol.* **2021**, *286*, 106085. [CrossRef]
32. Song, D.; Chen, Z.; Dong, L.; Zhu, W. Numerical investigation on dynamic response characteristics and deformation mechanism of a bedded rock mass slope subject to earthquake excitation. *Appl. Sci.* **2021**, *11*, 7068. [CrossRef]

33. Lenti, L.; Martino, S. The interaction of seismic waves with step-like slopes and its influence on landslide movements. *Eng. Geol.* **2012**, *126*, 19–36. [CrossRef]
34. Song, D.Q.; Che, A.L.; Zhu, R.; Ge, X.R. Natural Frequency Characteristics of Rock Masses Containing a Complex Geological Structure and Their Effects on the Dynamic Stability of Slopes. *Rock Mech. Rock Eng.* **2019**, *52*, 4457–4473. [CrossRef]
35. Li, J.; Law, S.S.; Ding, Y. Substructure damage identification based on response reconstruction in frequency domain and model updating. *Eng. Struct.* **2012**, *41*, 270–284. [CrossRef]
36. Yong, R.; Ye, J.; Li, B.; Du, S.G. Determining the maximum sampling interval in rock joint roughness measurements using Fourier series. *Int. J. Rock Mech. Min. Sci.* **2018**, *101*, 78–88. [CrossRef]
37. Chen, Z.; Xu, Q.; Hu, X. Study on dynamic response of the "Dualistic" structure rock slope with seismic wave theory. *J. Mt. Sci.* **2013**, *10*, 996–1007. [CrossRef]
38. Fan, G.; Zhang, L.M.; Zhang, J.J.; Ouyang, F. Energy-Based Analysis of Mechanisms of Earthquake-Induced Landslide Using Hilbert-Huang Transform and Marginal Spectrum. *Rock Mech. Rock Eng.* **2017**, *50*, 2425–2441. [CrossRef]
39. Yang, C.; Zhang, J.; Bi, J. Application of Hilbert-Huang Transform to the analysis of the landslides triggered by the Wenchuan earthquake. *J. Mt. Sci.* **2015**, *12*, 711–720. [CrossRef]
40. Reale, C.; Gavin, K.; Prendergast, L.J.; Xue, J. Multi-modal reliability analysis of slope stability. *Transp. Res. Proc.* **2016**, *14*, 2468–2476. [CrossRef]
41. Ahmed, N.; Rao, K.R. Fast Fourier Transform. In *Orthogonal Transforms for Digital Signal Processing*; Springer: Berlin/Heidelberg, Germany, 1975.
42. Zhang, Y.P. HHT Analysis of Blasting Vibration and Its Application. Ph.D. Thesis, Central South University, Changsha, China, 2006.
43. Huang, N.E.; Shen, Z.; Long, S.R.; Wu, M.C.; Shih, H.H.; Zheng, Q.; Yen, N.C.; Tung, C.C.; Liu, H.H. The empirical mode decomposition and the Hilbert spectrum for nonlinear and non-stationary time series analysis. *Proc. Math. Phys. Eng. Sci.* **1998**, *454*, 903–995. [CrossRef]
44. Huang, N.E.; Shen, Z.; Long, S.R. A new view of nonlinear water waves: The Hilbert spectrum. *Annu. Rev. Fluid Mech.* **1999**, *31*, 417–457. [CrossRef]
45. Pang, R.; Xu, B.; Zhou, Y.; Song, L. Seismic time-history response and system reliability analysis of slopes considering uncertainty of multi-parameters and earthquake excitations. *Comput. Geotech.* **2021**, *136*, 104245. [CrossRef]
46. Pilarska, D.; Maleska, T. Numerical Analysis of Steel Geodesic Dome under Seismic Excitations. *Materials* **2021**, *14*, 4493. [CrossRef]
47. Labanda, N.A.; Sottile, M.G.; Cueto, L.A.; Sfriso, A.O. Screening of seismic records to perform time-history dynamic analyses of tailings dams: A power-spectral based approach. *Soil Dyn. Earthq. Eng.* **2021**, *146*, 106750. [CrossRef]
48. Kostinakis, K.G.; Athanatopoulou, A.M.; Avramidis, I.E. Sectional forces for seismic design of R/C frames by linear time history analysis and application to 3D single-story buildings. *Soil Dyn. Earthq. Eng.* **2011**, *31*, 318–333. [CrossRef]